# Dynamics of Zonal Flows in Helical Systems

H. Sugama and T.-H. Watanabe

*National Institute for Fusion Science, Graduate University for Advanced Studies, Toki 509-5292, Japan*

(Received 16 December 2004; published 22 March 2005)

A theory for describing collisionless long-time behavior of zonal flows in helical systems is presented and its validity is verified by gyrokinetic-Vlasov simulation. It is shown that, under the influence of particles trapped in helical ripples, the response of zonal flows to a given source becomes weaker for lower radial wave numbers and deeper helical ripples while a high-level zonal-flow response, which is not affected by helical-ripple-trapped particles, can be maintained for a longer time by reducing their bounce-averaged radial drift velocity. This implies a possibility that helical configurations optimized for reducing neoclassical ripple transport can simultaneously enhance zonal flows which lower anomalous transport.

DOI: 10.1103/PhysRevLett.94.115001 PACS numbers: 52.55.Hc, 52.25.Fi, 52.35.Ra, 52.65.Tt

Zonal flows are observed in numerous natural systems such as atmospheric currents, while in fusion science they are intensively investigated as an attractive mechanism for realizing a good plasma confinement [1]. Rosenbluth and Hinton [2] showed that initial $\mathbf{E}\times\mathbf{B}$ rotation in tokamaks is not fully damped by collisionless processes, but it approaches a finite value. Collisional decay of zonal flows occurs in the long course of time [3] although the residual zonal flows in a collisionless time scale still influence the turbulent transport. Since zonal flows are a key issue for improved confinement in helical systems as well [4,5], it is necessary to examine how helical geometries affect zonal-flow damping. In the present work, collisionless zonal-flow dynamics in helical systems is investigated. In the same manner as in Rosenbluth and Hinton [2], we here treat the ion-temperature-gradient (ITG) turbulence [6] as a known source and analytically derive the response kernel which relates the zonal-flow potential to the source and also represents dependence on an initially given zonal flow. We also verify the validity of the derived response kernel by a recently developed gyrokinetic-Vlasov-simulation code [7].

In helical configurations, the radial drift motion of particles trapped in helical ripples yields neoclassical ripple transport in the weak collisionality regime [8,9]. We show that this radial drift also causes a significant difference between long-time zonal-flow behavior in helical systems and that in tokamaks. It is observed in the large helical device (LHD) [10] that not only neoclassical but also anomalous transport is reduced by the inward shift of the magnetic axis which decreases the radial drift of helical-ripple-trapped particles but increases the unfavorable magnetic curvature to destabilize pressure-gradient-driven instabilities such as the ITG mode [11–13]. Our study suggests that helical configurations optimized for reduction of the neoclassical ripple transport may simultaneously lower the anomalous transport through enhancing the zonal-flow level.

We use the toroidal coordinates $(r, \theta, \zeta)$, where $r$, $\theta$, and $\zeta$ denote the flux-surface label, the poloidal angle, and the toroidal angle, respectively. The magnetic field is written as $\mathbf{B} = \nabla\psi(r)\times\nabla(\theta - \zeta/q(r))$, where $2\pi\psi(r)$ is equal to the toroidal flux within the flux surface labeled $r$ and $q(r)$ represents the safety factor. Following Shaing and Hokin [9], we here consider helical systems with the magnetic field strength written by a function of poloidal and toroidal angles (its $r$ dependence is not shown here for simplicity) as $B = B_0[1 - \epsilon_{10}\cos\theta - \epsilon_{L0}\cos(L\theta) - \sum_{n=0,\pm1,\ldots}\epsilon_h^{(n)}\times\cos\{(L+n)\theta - M\zeta\}] = B_0[1 - \epsilon_T(\theta) - \epsilon_H(\theta)\cos\{L\theta - M\zeta + \chi_H(\theta)\}]$, where $\epsilon_T(\theta) = \epsilon_{10}\cos\theta + \epsilon_{L0}\cos(L\theta)$, $\epsilon_H(\theta) = \sqrt{C^2(\theta) + D^2(\theta)}$, $\chi_H(\theta) = \arctan[D(\theta)/C(\theta)]$, $C(\theta) = \sum_{n=0,\pm1,\ldots}\epsilon_h^{(n)}\cos(n\theta)$, $D(\theta) = \sum_{n=\pm1,\ldots}\epsilon_h^{(n)}\times\sin(n\theta)$, and $M$ $(L)$ is the toroidal (main poloidal) period number of the helical field. For the LHD, $L = 2$ and $M = 10$. Here, we assume that $l/(qM) \ll 1$. Multiple-helicity effects can be included in the function $\epsilon_H(\theta)$.

The gyrokinetic equation [14] for the zonal-flow component with the perpendicular wave number vector $\mathbf{k}_\perp = k_r\nabla r$ is given by

$$\left(\frac{\partial}{\partial t} + v_\parallel\mathbf{b}\cdot\nabla + i\omega_D\right)g_{\mathbf{k}_\perp} = \frac{e}{T}F_0J_0(k_\perp\rho)\frac{\partial\phi_{\mathbf{k}_\perp}}{\partial t} + S_{\mathbf{k}_\perp}F_0, \tag{1}$$

where $J_0(k_\perp\rho)$ is the zeroth-order Bessel function, $\rho = v_\perp/\Omega$ is the gyroradius, and $\Omega = eB/(mc)$ is the gyrofrequency. Here, subscripts to represent particle species are dropped for simplicity. The equilibrium distribution function $F_0$ is assumed to be given by the local Maxwellian and the perturbed particle distribution function $\delta f \equiv f - F_0$ is written in terms of the electrostatic potential $\phi$ and the solution $g$ of Eq. (1) as $\delta f = -(e\phi/T)F_0 + g\exp(-i\mathbf{k}_\perp\cdot\boldsymbol{\rho})$, where $\boldsymbol{\rho} = \mathbf{b}\times\mathbf{v}/\Omega$. The drift frequency $\omega_D$ is defined by $\omega_D \equiv \mathbf{k}_\perp\cdot\mathbf{v}_d \equiv k_r v_{dr}$, where $v_{dr} = \mathbf{v}_d\cdot\nabla r$ is the radial component of the guiding-center drift velocity. The source term $S_{\mathbf{k}_\perp}F_0$ on the right-hand side of Eq. (1) represents the $\mathbf{E}\times\mathbf{B}$ nonlinearity and is written as $S_{\mathbf{k}_\perp}F_0 = (c/B)\sum_{\mathbf{k}'_\perp+\mathbf{k}''_\perp=\mathbf{k}_\perp}[\mathbf{b}\cdot(\mathbf{k}'_\perp\times\mathbf{k}''_\perp)]J_0(k'_\perp\rho)\phi_{\mathbf{k}'_\perp}g_{\mathbf{k}''_\perp}$.

 

The trapping parameter $\kappa$ is defined by $\kappa^2 = [1 - \lambda B_0\{1 - \epsilon_T(\theta) - \epsilon_H(\theta)\}]/[2\lambda B_0 \epsilon_H(\theta)]$ with $\lambda \equiv \mu/w$, where $w \equiv \frac{1}{2}mv^2$ and $\mu \equiv mv_\perp^2/(2B)$ represent the kinetic energy and the magnetic moment, respectively. Then, particles trapped in helical ripples are characterized by $\kappa^2 < 1$. Using $l/(qM) \ll 1$, we approximate the field line element $dl$ by $R_0 d\zeta$, where $R_0$ denotes the major radius of the toroid. Then, the orbital average within a helical ripple is defined by $\overline{A} = \int (R_0 d\zeta/|v_\parallel|)A/\tau_h$, where $\tau_h = \int (R_0 d\zeta/|v_\parallel|)$; for $\kappa^2 < 1$, the integral $\int d\zeta$ goes over a closed orbit while, for $\kappa^2 > 1$, it goes a whole helical ripple. Using the longitudinal adiabatic invariant $J$ [9] given by $J = 16(R_0/M)(\mu B_0 \epsilon_H/m)^{1/2} \times [E(\kappa) - (1-\kappa^2)K(\kappa)]$ for $\kappa^2 < 1$ and $J = 8(R_0/M) \times (\mu B_0 \epsilon_H/m)^{1/2} \kappa E(\kappa^{-1})$ for $\kappa^2 > 1$ with the complete elliptic integrals $K(\kappa)$ and $E(\kappa)$, the orbital average of the radial drift velocity within a helical ripple is given by $\overline{v}_{dr} = (mc/e\psi'\tau_h)(\partial J/\partial \theta)$, where $\psi' = d\psi/dr$ and $\tau_h = m(\partial J/\partial w)$. The drift frequency $\omega_D$ is expressed as $\omega_D \equiv k_r(\overline{v}_{dr} + v_\parallel \mathbf{b}\cdot\nabla\delta_r)$, where $\delta_r = \int^l (dl/v_\parallel)(v_{dr} - \overline{v}_{dr})$ represents the radial displacement of the guiding center from the helical-ripple-averaged radial position. Then, Eq. (1) is rewritten as

$$\left(\frac{\partial}{\partial t} + v_\parallel \mathbf{b}\cdot\nabla + ik_r\overline{v}_{dr}\right)(g_{\mathbf{k}_\perp} e^{ik_r\delta_r}) = \frac{e}{T}F_0 e^{ik_r\delta_r} J_0 \frac{\partial \phi_{\mathbf{k}_\perp}}{\partial t} + e^{ik_r\delta_r} S_{\mathbf{k}_\perp} F_0. \tag{2}$$

We here consider the long-time behavior of zonal flows. Then, in Eq. (2), the time-derivative terms, the radial guiding-center drift term, and the source term are smaller than the parallel streaming term such that they are regarded as of the higher order. The parallel derivative is rewritten as $\mathbf{b}\cdot\nabla \simeq R_0^{-1}(\partial/\partial\zeta + q^{-1}\partial/\partial\theta)$. Here, we treat the poloidal field as a higher-order quantity than the toroidal field. Based on these orderings, we expand $g_{\mathbf{k}_\perp} e^{ik_r\delta_r}$ as $g_{\mathbf{k}_\perp} e^{ik_r\delta_r} = h_0 + h_1 + \cdots$ and obtain the lowest-order equation $(v_\parallel/R_0)(\partial h_0/\partial\zeta) = 0$ from Eq. (2). Thus, we can write $h_0 = h_0(t, r, \theta, w, \mu, \sigma)$, where the dependence on $\sigma = v_\parallel/|v_\parallel|$ disappears for $\kappa^2 < 1$. The first-order equation is written as

$$\frac{v_\parallel}{R_0}\frac{\partial h_1}{\partial \zeta} = -\left(\frac{\partial}{\partial t} + \frac{v_\parallel}{R_0 q}\frac{\partial}{\partial \theta} + ik_r\overline{v}_{dr}\right)h_0 + \frac{e}{T}F_0 e^{ik_r\delta_r} J_0 \frac{\partial \phi_{\mathbf{k}_\perp}}{\partial t} + e^{ik_r\delta_r} S_{\mathbf{k}_\perp} F_0. \tag{3}$$

For particles trapped in a helical ripple ($\kappa^2 < 1$), the orbital average of Eq. (3) and its time integral yield

$$h_0(t) = h_0(0)e^{-ik_r\overline{v}_{dr}t} + \int_0^t dt' e^{-ik_r\overline{v}_{dr}(t-t')} F_0\left[\frac{e}{T}\overline{\left(e^{ik_r\delta_r} J_0 \frac{\partial \phi_{\mathbf{k}_\perp}(t')}{\partial t'}\right)} + \overline{(e^{ik_r\delta_r} S_{\mathbf{k}_\perp}(t'))}\right]. \tag{4}$$

When $\kappa^2 > 1$, using the periodic condition $h_1(\zeta + 2\pi/M) = h_1(\zeta)$ and taking the orbital average of Eq. (3) within a helical ripple give

$$\left(\frac{\partial}{\partial t} + \omega_\theta \frac{\partial}{\partial \theta}\right)(e^{ik_r\Delta_r} h_0) = e^{ik_r\Delta_r} F_0\left[\frac{e}{T}\overline{\left(e^{ik_r\delta_r} J_0 \frac{\partial \phi_{\mathbf{k}_\perp}}{\partial t}\right)} + \overline{(e^{ik_r\delta_r} S_{\mathbf{k}_\perp})}\right], \tag{5}$$

where $\omega_\theta = 2\pi\sigma/(qM\tau_h)$ is the helical-ripple-averaged poloidal angular velocity and $\Delta_r = \sigma(qM/2\pi)(mc/e\psi')(J - J_t)$ with $J_t$ defined later represents the radial displacement of the helical-ripple-averaged guiding-center position. For $\kappa^2 > 1$, particles are classified into two types, particles trapped by the toroidicity and passing particles. For these particles, we regard $\omega_\theta \partial(e^{ik_r\Delta_r} h_0)/\partial\theta$ as a dominant term in Eq. (5) based on the long-time ordering and expand $e^{ik_r\Delta_r} h_0$ as $e^{ik_r\Delta_r} h_0 = \eta_0 + \eta_1 + \cdots$, where $\eta_0$ is independent of $\theta$ because it satisfies the lowest-order equation $\omega_\theta \partial\eta_0/\partial\theta = 0$. The solubility condition for $\eta_1$ is derived from Eq. (5) and integrated in time to give

$$\eta_0(t) = \eta_0(0) - \frac{e}{T}F_0\langle e^{ik_r\Delta_r}\overline{(e^{ik_r\delta_r} J_0 \phi_{\mathbf{k}_\perp}(0))}\rangle_{\rm po} + F_0\left\langle e^{ik_r\Delta_r}\overline{\left[e^{ik_r\delta_r}\left\{J_0\frac{e\phi_{\mathbf{k}_\perp}(t)}{T} + R_{\mathbf{k}_\perp}(t)\right\}\right]}\right\rangle_{\rm po}, \tag{6}$$

where $R_{\mathbf{k}_\perp}(t) \equiv \int_0^t dt' S_{\mathbf{k}_\perp}(t')$ and the poloidal-orbit average $\langle A\rangle_{\rm po}$ is defined by $\langle A\rangle_{\rm po} = \frac{1}{2}\sum_{\sigma=\pm1} \times \int_{-\theta_t}^{\theta_t}(d\theta/|\omega_\theta|)A/\int_{-\theta_t}^{\theta_t}(d\theta/|\omega_\theta|)$ for toroidally trapped particles and $\langle A\rangle_{\rm po} = \int_0^{2\pi}(d\theta/|\omega_\theta|)A/\int_0^{2\pi}(d\theta/|\omega_\theta|)$ for passing particles with $\theta_t$ given by the condition $\kappa(\theta = \theta_t) = 1$ which is equivalent to $\omega_\theta(\theta = \theta_t) = 0$. Now, $J_t$ is defined by $J_t = J(\theta = \theta_t)$ for toroidally trapped particles and by $J_t = J(\theta = \pi)$ for passing particles.

The electrostatic potential $\phi_{\mathbf{k}_\perp}$ is determined by the quasineutrality condition, $-n_0 e\phi_{\mathbf{k}_\perp}/T_i + \int d^3v J_0 g_{i\mathbf{k}_\perp} = n_0 e\phi_{\mathbf{k}_\perp}/T_e + \int d^3v g_{e\mathbf{k}_\perp}$, where the small electron gyroradius limit $k_\perp\rho_e \to 0$ is considered. In the lowest order of the long-time ordering, we substitute Eq. (4) into $g_{\mathbf{k}_\perp} = e^{-ik_r\delta_r}h_0$ for $\kappa^2 < 1$ and Eq. (6) into $g_{\mathbf{k}_\perp} = e^{-ik_r\delta_r}e^{-ik_r\Delta_r}\eta_0$ for $\kappa^2 > 1$ in order to evaluate the nonadiabatic parts of the density perturbations. We find from Eq. (4) that effects of $\overline{v}_{dr}$ on the density of helical-ripple-trapped particles strongly depend on time $t$. Let us define a characteristic transition time $\tau_c$ by $\tau_c \sim 1/|k_r\overline{v}_{dr}|$, where $\overline{v}_{dr}$ is evaluated by considering helical-ripple-trapped thermal particles with $\mu B_0 \sim T$, $\kappa \sim 1$, and $\theta \sim \pi/2$.

When $t \ll \tau_c$, effects of $\overline{v}_{dr}$ are weak and the quasineutrality condition is written as

$$n_0 e\left(\frac{1}{T_i}+\frac{1}{T_e}\right)\phi_{\mathbf{k}_\perp}(t) - \frac{e}{T_i}\int_{\kappa^2<1} d^3v F_{i0} J_0 e^{-ik_r\delta_r}\overline{(e^{ik_r\delta_r}J_0\phi_{\mathbf{k}_\perp}(t))} - \frac{e}{T_i}\int_{\kappa^2>1} d^3v F_{i0} e^{-ik_r\Delta_r}e^{-ik_r\delta_r}J_0\langle e^{ik_r\Delta_r}\overline{(e^{ik_r\delta_r}J_0\phi_{\mathbf{k}_\perp}(t))}\rangle_{\mathrm{po}} - \frac{e}{T_e}\int_{\kappa^2<1} d^3v F_{e0}\overline{\phi_{\mathbf{k}_\perp}(t)} - \frac{e}{T_e}\int_{\kappa^2>1} d^3v F_{e0}\langle\overline{\phi_{\mathbf{k}_\perp}(t)}\rangle_{\mathrm{po}} = \sigma_<, \quad (7)$$

where $\sigma_<$ is given by the initial values $\phi_{\mathbf{k}_\perp}(0)$, $h_0(0)$, and $\eta_0(0)$ as well as the time integral of the $\mathbf{E}\times\mathbf{B}$ nonlinear source terms $R_{\mathbf{k}_\perp}(t) = \int_0^t dt' S_{\mathbf{k}_\perp}(t')$. Here, the radial displacement of the electron guiding center is neglected because of the small electron mass. Representing Eq. (7) by $\mathcal{L}\phi_{\mathbf{k}_\perp} = \sigma_<$ and defining the Hermitian inner product by $(u, v) \equiv \langle u^* v\rangle$, where $\langle\cdot\rangle$ denotes the flux-surface average, we find that the operator $\mathcal{L}$ is self-adjoint, $(u, \mathcal{L}v) = (\mathcal{L}u, v)$, and that $(u, \mathcal{L}u) \geq 0$. Then, the variational principle for $\mathcal{L}\phi_{\mathbf{k}_\perp} = \sigma_<$ is given by $\delta V = 0$, where $V \equiv (\phi_{\mathbf{k}_\perp}, \mathcal{L}\phi_{\mathbf{k}_\perp})/|(\phi_{\mathbf{k}_\perp}, \sigma_<\phi_{\mathbf{k}_\perp})|^2$.

Now, we assume $k_\perp\rho$ and $k_r\Delta_r$ to be small and use them as expansion parameters. We neglect $k_r\delta_r$ because generally $\delta_r$ is much smaller than $\rho$. The source $\sigma_<$ is considered to be of order $k_\perp^2\rho^2$. Then, from the lowest-order equation $(\phi_{\mathbf{k}_\perp}, \mathcal{L}_0\phi_{\mathbf{k}_\perp}) = 0$, we can show that $\phi_{\mathbf{k}_\perp}$ is a flux-surface function, $\partial\phi_{\mathbf{k}_\perp}/\partial\zeta = \partial\phi_{\mathbf{k}_\perp}/\partial\theta = 0$. The next-order equation $(\phi_{\mathbf{k}_\perp}, \mathcal{L}_1\phi_{\mathbf{k}_\perp}) = (\phi_{\mathbf{k}_\perp}, \sigma_<)$ gives $e\phi_{\mathbf{k}_\perp}/T_i = \langle\sigma_<\rangle/\mathcal{D}_<$, where $\mathcal{D}_< = \langle\int d^3v F_{i0}[\frac{1}{2}k_\perp^2\rho^2 + k_r^2\{\langle\Delta_r^2\rangle_{\mathrm{po}} - \langle\Delta_r\rangle_{\mathrm{po}}^2\}H(\kappa^2-1)]\rangle$ and $H(x) = 1$ (for $x > 0$), 0 (for $x < 0$). Here, the second group of terms in the integrand represent the neoclassical polarization effect due to toroidally trapped particles with $\kappa^2 > 1$.

To the lowest order in $k_\perp^2\rho^2$, electron contributions to $\sigma_<$ are neglected. The initial values $h_{i0}(0)$ and $\eta_{i0}$ in Eq. (7) are given by $h_{i0}(0) = \overline{e^{ik_r\delta_r}g_{i\mathbf{k}_\perp}(0)}$ and $\eta_{i0}(0) = \langle e^{ik_r\Delta_r}\overline{(e^{ik_r\delta_r}g_{i\mathbf{k}_\perp}(0))}\rangle_{\mathrm{po}}$. We assume the initial perturbed ion gyrocenter distribution function to take the Maxwellian form, $\delta f_{i\mathbf{k}_\perp}^{(\mathrm{gyro})}(0) \equiv -J_0(e\phi_{\mathbf{k}_\perp}(0)/T_i)F_{i0} + g_{i\mathbf{k}_\perp}(0) = (\delta n_{i\mathbf{k}_\perp}^{(\mathrm{gyro})}(0)/n_0)F_{i0}$. The quasineutrality condition gives $\delta n_{i\mathbf{k}_\perp}^{(\mathrm{gyro})}(0) = n_0(k_\perp^2 a_i^2)(e\phi_{\mathbf{k}_\perp}(0)/T_i)$ with $a_i^2 = T_i/(m_i\Omega_i^2)$. Then, we obtain $\langle\sigma_<\rangle = n_0\langle k_\perp^2 a_i^2\rangle e\phi_{\mathbf{k}_\perp}(0)/T_i + \langle\int d^3v F_{i0}R_{i\mathbf{k}_\perp}(t)\rangle$ and the long-time behavior of the zonal-flow potential for $t \ll \tau_c$,

$$\frac{e\phi_{\mathbf{k}_\perp}(t)}{T_i} = \mathcal{K}_<\left[\frac{e\phi_{\mathbf{k}_\perp}(0)}{T_i} + \frac{\int_0^t dt'\langle\int d^3v F_{i0}S_{i\mathbf{k}_\perp}(t')\rangle}{n_0\langle k_\perp^2 a_i^2\rangle}\right], \quad (8)$$

where the response kernel for $t \ll \tau_c$ is represented by

$$\mathcal{K}_< = 1/(1+G) \quad (9)$$

and

$$G = \frac{12}{\pi^3}B_0R_0^2q^2\left\langle\frac{B^2}{|\nabla\psi|^2}\right\rangle\left[\int_0^{1/B_M} d\lambda \oint\frac{d\theta}{2\pi}(2\lambda B_0\epsilon_H)^{-1/2}\kappa^{-1}K(\kappa^{-1})\left\{(2\lambda B_0\epsilon_H)^{1/2}\kappa E(\kappa^{-1}) - \frac{\oint\frac{d\theta}{2\pi}K(\kappa^{-1})E(\kappa^{-1})}{\oint\frac{d\theta}{2\pi}(2\lambda B_0\epsilon_H)^{-1/2}\kappa^{-1}K(\kappa^{-1})}\right\}^2 + \int_{1/B_M}^{1/B'_m} d\lambda\int_{\kappa^2(\theta)>1}\frac{d\theta}{2\pi}(2\lambda B_0\epsilon_H)^{1/2}\kappa K(\kappa^{-1})\left\{E(\kappa^{-1}) - \frac{1}{\kappa}\left(\frac{\epsilon_H(\theta_t)}{\epsilon_H}\right)^{1/2}\right\}^2\right]. \quad (10)$$

The geometrical factor $G$ measures the ratio of the neoclassical polarization due to toroidally trapped particles to the classical polarization. Here $B_M$ denotes the maximum field strength over the flux surface and $B'_m$ represents the minimum value of local maximum field strengths within each helical ripple.

Next, when $t \gg \tau_c$, the density of nonadiabatic helical-ripple-trapped particles is strongly damped because of phase mixing caused by the bounce-averaged radial drift motion [see Eq. (4)]. Then, the quasineutrality condition is given by Eq. (7) with the velocity-space integrals over the $\kappa^2 < 1$ region dropped. Employing the same procedures used in deriving Eqs. (8)–(10), $\phi_{\mathbf{k}_\perp}$ is shown to be again a flux-surface function to the lowest order in $k_\perp^2\rho^2$ and $\epsilon_H^{1/2}$, and we obtain $e\phi_{\mathbf{k}_\perp}/T_i = \langle\sigma_>\rangle/\mathcal{D}_>$, where $\mathcal{D}_> \equiv \mathcal{D}_< + (2/\pi)(1 - \langle k_\perp^2 a_i^2\rangle + T_i/T_e)\langle(2\epsilon_H)^{1/2}\rangle$ and $\langle\sigma_>\rangle \equiv \langle\sigma_<\rangle - (2/\pi)\langle(2\epsilon_H)^{1/2}\rangle\langle k_\perp^2 a_i^2\rangle[n_0 e\phi_{\mathbf{k}_\perp}(0)/T_i]$. Finally, the long-time behavior of the zonal-flow potential for $t \gg \tau_c$ is given by

$$\frac{e\phi_{\mathbf{k}_\perp}(t)}{T_i} = \mathcal{K}_>\left[\frac{e\phi_{\mathbf{k}_\perp}(0)}{T_i} + \frac{\int_0^t dt'\langle\int_{\kappa^2>1} d^3v F_{i0}S_{i\mathbf{k}_\perp}(t')\rangle}{n_0\langle k_\perp^2 a_i^2\rangle\{1 - (2/\pi)\langle(2\epsilon_H)^{1/2}\rangle\}}\right] \quad (11)$$

and

$$\mathcal{K}_> = \langle k_\perp^2 a_i^2\rangle[1 - (2/\pi)\langle(2\epsilon_H)^{1/2}\rangle] \times \{\langle k_\perp^2 a_i^2\rangle[1 - (2/\pi)\langle(2\epsilon_H)^{1/2}\rangle + G] + (2/\pi)(1 + T_i/T_e)\langle(2\epsilon_H)^{1/2}\rangle\}^{-1}. \quad (12)$$

Here, terms proportional to $\langle(2\epsilon_H)^{1/2}\rangle$ are derived from suppressing the density perturbations of the nonadiabatic helical-ripple-trapped particles. A term with $T_i/T_e$ appears in the response kernel $\mathcal{K}_>$ for $t \gg \tau_c$ because not only ions but also electrons influence the quasineutrality condition through their helical-ripple-bounce-averaged radial drift motion. The dependence on electrons and on the radial wave number shown in Eq. (12) is not seen in the

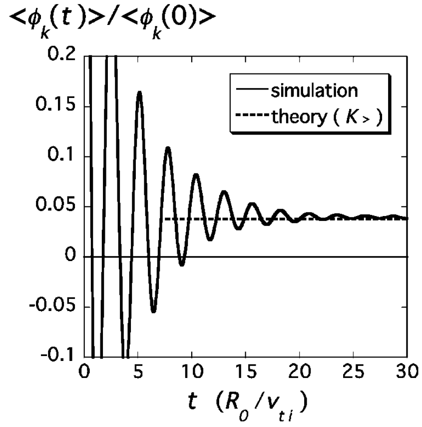


FIG. 1. Time evolution of the zonal-flow potential obtained by the gyrokinetic-Vlasov simulation for a helical system with $L = 2$, $M = 10$, $q = 1.5$, $\epsilon_t = \epsilon_h = 0.1$, and $k_r a_i = 0.131$. A dashed horizontal line corresponds to $\mathcal{K}_>$ given by Eq. (12) for $t > \tau_c$.

tokamak case. In the axisymmetric limit $\epsilon_H \rightarrow +0$ with $\epsilon_T = \epsilon_t \cos\theta$, we obtain $G \rightarrow 1.6q^2/\epsilon_t^{1/2}$, which reduces both Eqs. (9) and (12) to the Rosenbluth-Hinton formula $\mathcal{K}_{\text{R-H}} = 1/(1 + 1.6q^2/\epsilon_t^{1/2})$ [2].

In order to examine the analytical results shown above, a linearized ion gyrokinetic equation combined with the quasineutrality condition is numerically solved by a toroidal flux-tube gyrokinetic-Vlasov code [7]. Since the perturbed electron density is simply calculated by using $n_{e\mathbf{k}_\perp} = (n_0 e/T_e)(\phi_{\mathbf{k}_\perp} - \langle\phi_{\mathbf{k}_\perp}\rangle)$ in our simulations, the term proportional to $T_i/T_e$ in Eq. (12) should be dropped when comparing that formula with the simulation results. Here, we consider the $L = 2/M = 10$ single-helicity case, in which $\epsilon_h^{(n\neq 0)} = 0$ and therefore $\epsilon_H = \epsilon_h^{(0)} \equiv \epsilon_h$ is independent of $\theta$. We also put $\epsilon_t \equiv \epsilon_{10}$ and $\epsilon_{L0} = 0$ so that $\epsilon_T = \epsilon_t \cos\theta$. The initial perturbed ion gyrocenter distribution function is given by the Maxwellian form. We define the radial coordinate $r$ by $\psi = B_0 r^2/2$ and use $\overline{v}_{dr} = -(c\mu/eR_0)\sin\theta$, $\langle k_\perp^2 a_i^2\rangle \simeq k_r^2 a_i^2$, and $\tau_c \simeq (k_r c T_i/eB_0 R_0)^{-1} = (R_0/v_{ti})/(k_r a_i)$, where $a_i \simeq v_{ti}/\Omega_{i0}$, $\Omega_{i0} = eB_0/(m_i c)$, and $v_{ti} = (T_i/m_i)^{1/2}$.

Time evolution of the zonal-flow potential obtained by the simulation is plotted by a solid curve in Fig. 1, where $\epsilon_t = 0.1$, $\epsilon_h = 0.1$, $q = 1.5$, and $k_r a_i = 0.131$ are used. Here, a dashed horizontal line represents the response kernel $\mathcal{K}_>$ given by Eq. (12) for $t > \tau_c(= 7.6R_0 v_{ti})$. It is seen that, after oscillations of the geodesic acoustic mode (GAM) [15] are damped, the zonal-flow amplitude approaches the predicted value $\mathcal{K}_> = 0.038$, which is smaller than $\mathcal{K}_< = 0.39$ and $\mathcal{K}_{\text{R-H}} = 0.081$ for the used parameters. Under the conditions used in our simulation, the GAM oscillations dominate the zonal-flow evolution for $t < \tau_c$ so that we cannot identify $\mathcal{K}_<$ given by Eq. (8) which describes the long-time behavior for $t \ll \tau_c$ with rapid phenomena such as the GAM neglected. It is confirmed from other simulations for $k_r a_i = 0.0654$, 0.131, 0.196 and $\epsilon_h = 0.05$, 0.1, 0.2 that Eq. (12) agrees with the long-time limit of $\langle\phi_{\mathbf{k}_\perp}(t)\rangle/\langle\phi_{\mathbf{k}_\perp}(0)\rangle$ obtained by the simulations within an error of about 15% at most. A better agreement between the simulation and theoretical results is verified for lower $k_r a_i$ and smaller $\epsilon_h$ because these parameters are assumed to be small in deriving the analytical results.

In conclusion, we have shown how the collisionless long-time behavior of zonal flows in helical systems is influenced by the bounce-averaged radial drift motion of helical-ripple-trapped particles. It is predicted that, under the influence of helical-ripple-trapped particles, for the lower radial wave numbers, the long-time limit of the zonal-flow potential amplitude becomes smaller although simultaneously the characteristic transition time $\tau_c(\sim 1/k_r|\overline{v}_{dr}|)$ becomes longer. In some optimized helical configurations such as quasipoloidally symmetric systems [16,17],which significantly reduce neoclassical transport by suppressing both $|\overline{v}_{dr}|$ and $G$, we expect the response kernels $\mathcal{K}_>$, $\mathcal{K}_<$, and $\tau_c$ to increase such that large zonal flows can be maintained for a long-time period, which contribute to a reduction of anomalous transport as well.

The authors thank Dr. M. Yokoyama and Dr. Y. Idomura for helpful discussions. This work is supported in part by the Japanese Ministry of Education, Culture, Sports, Science, and Technology, Grants No. 16560727 and No. 14780387.


[1] P. H. Diamond *et al.*, in Proceedings of the 20th IAEA Fusion Energy Conference, Vilamoura, Portugal, 2004, OV/2-1 (to be published).
[2] M. N. Rosenbluth and F. L. Hinton, Phys. Rev. Lett. **80**, 724 (1998).
[3] F. L. Hinton and M. N. Rosenbluth, Plasma Phys. Controlled Fusion **41**, A653 (1999).
[4] A. Fujisawa *et al.*, Phys. Rev. Lett. **93**, 165002 (2004).
[5] A. Hasegawa and M. Wakatani, Phys. Rev. Lett. **59**, 1581 (1987); H. Sugama, M. Wakatani, and A. Hasegawa, Phys. Fluids **31**, 1601 (1988).
[6] W. Horton, Rev. Mod. Phys. **71**, 735 (1999).
[7] T.-H. Watanabe and H. Sugama, in 20th IAEA Fusion Energy Conference, Vilamoura, Portugal, 2004, TH/8-3Rb (Ref. [1]).
[8] M. Wakatani, *Stellarator and Heliotron Devices* (Oxford University Press, Oxford, 1998), Chap. 7.
[9] K. C. Shaing and S. A. Hokin, Phys. Fluids **26**, 2136 (1983).
[10] O. Motojima *et al.*, Nucl. Fusion **43**, 1674 (2003).
[11] H. Yamada *et al.*, Plasma Phys. Controlled Fusion **43**, A55 (2001).
[12] T. Kuroda and H. Sugama, J. Phys. Soc. Jpn. **70**, 2235 (2001).
[13] G. Rewoldt *et al.*, Nucl. Fusion **42**, 1047 (2002).
[14] E. A. Frieman and L. Chen, Phys. Fluids **25**, 502 (1982).
[15] N. Winsor, J. L. Johnson, and J. J. Dawson, Phys. Fluids **11**, 2448 (1968).
[16] D. A. Spong *et al.*, Nucl. Fusion **41**, 711 (2001).
[17] M. Yokoyama, J. Plasma Fusion Res. **78**, 205 (2002).